Supporting Information

Hicks et al. 10.1073/pnas.1019660108

SI Materials and Methods

Strains and Construction. JKM139 (*hoΔ hml::ADE1 MAT***a** *hmr::ADE1 ade3::GAL10::HO*) was previously described (1). JKM179 (*hoΔ hml::ADE1 MATα hmr::ADE1 ade3::GAL10::HO*) was previously described (1). JKM161 (*hoΔ HMLα MAT***a** *hmr::ADE1 ade3::GAL10::HO*) was previously described (2). WH3 (*hoΔ HMLα MAT***a** *hmr::ADE1 ade3::GAL10::HO rdh54::URA3*) was created by transforming JKM161 with a *URA3-MX* fragment PCR amplified from p4348 (3) using primers Rdh54-KMXp1 (5′-**CTCGGTATATCAAACGGTATTTGATTCCGGTACTACTCAA-**gatatcaagcttgcctcgtccccgc-3′), which contains 40 bp (uppercase bold) of homology with the nt 63–102 of the *RDH54* ORF, and Rdh54-KMXp2 (5′-**ATAGCTATTTTATTTAGTATATAAGTGT-CCATATTTGGCG**gtcgacactggatggcggcgttagtatc-3′), which contains 40 bp (uppercase bold) of homology immediately downstream of the *RDH54* ORF. WH10 (*hoΔ HMLα MAT***a** *hmr::ADE1 ade3::GAL10::HO rad54::KANMX*) was created by transforming JKM161 with a *KAN-MX* fragment PCR amplified from M3927 (4) by primers Rad54-KMXp1 (5′-**AGCTCTATTTCA-AGGTACCATATATATTTCCTTATAACTG**gatatcaagcttgcctcgtc-cccgc-3′), which contains 40 bp (uppercase bold) of homology immediately upstream of the *RAD54* ORF, and Rad54-KMXp2 (5′-**ACTTTTTGTTTTTGTTTTATAAGTACATGTATGTAAGA-GA**gtcgacactggatggcggcgttagtatc-3′), which contains 40 bp (uppercase bold) of homology immediately downstream of the *RAD54* ORF. WH12 (*hoΔ HMLα MAT***a** *hmr::ADE1 ade3::GAL10::HO rad54::KANMX rdh54::URA3*) was created by tetrad dissection of a sporulated diploid created by mating WH3 (switched to *MAT*α) and WH10. WH219 (*hoΔ HMLα*(*W*/*X*::*URA3-MX*) *MAT***a** *DELhmr::ADE1 ade1-100 leu2, 3-112 lys5 trp1::hisG ura3-52 ade3::GAL10::HO*) was created by transforming JKM161 with a *URA3-MX* fragment PCR amplified from p4348 (3) using primers HMLD-MXp1 (5′-**CACATAGAATGAAATGTAAACAAAGATTTCAGAAA-AATCGTCATTCAAAC**gatatcaagcttgcctcgtccccgc-3′), which contains 50 bp (uppercase bold) of homology with the first 50 bp immediately upstream of the W-region at *HML* and HMLD-MXp3 (5′-**TTTTAAATCCACAAATCACAGATGAGTTTAAATC-CAGCATACTAGACATA**gtcgacactggatggcggcgttagtatc-3′), which contains 50 bp (uppercase bold) of homology with the first 50 bp of the Yα region at *HML*. WH229 (*hoΔ HMLα*(W&5′X::URA3-MX6) *MAT***a** *hmr::ADE1 ade3::GAL10::HO*) was constructed by transforming JKM161 with a PCR product of URA3-MX such that all of the W region and the first 378 bp of the X region (chromosome III coordinates 11509–12617) were deleted. The URA3-MX6 deletion cassette was amplified from p4348 (3) with primers HMLD-MXp1 (5′-**CACATAGAATGAAATGTAAACAA-AGATTTCAGAAAAATCGTCATTCAAAC**gatatcaagcttgcctcgtcc-ccgc-3′), which contains 50 bp (uppercase bold) of homology with the first 50 bp immediately upstream of the W-region at *HML* and HMLD-MXp2 (5′-**TGGTAACTCAAGATATGATAAA-CAAAAGTACTAAACCTTACAGAGGACAC**gtcgacactggatggcggc-gttagtatc-3′), which contains 50 bp (uppercase bold) of homology with nts 379–428 of the X region. WH259 (*HMLα*(*W*/ *X*::*URA3-MX*) *MAT***a** *hmr::ADE1 ade3::GAL10::HO rad54::LEU2*) was isolated by tetrad dissection of a sporulated diploid created by mating WH219 to JKM128 (*hml::ADE1 MATα hmr::ADE1 rad54::LEU2*). MY121 (*HMLα MAT***a** *hmr::ADE1 cdc7-as3 ade3::GAL-HO*) was created by tetrad dissection of a sporulated diploid created by mating ECY413 (*MATα HMLα HMR*α-BamHI *ade3::GAL-HO cdc7-as3*) to MY083 (*HMLα MAT***a** *hmr::ADE1 ade3::GAL-HO dpb11-1*). MY122 (*HMLα MAT***a** *Δhmr::ADE1 cdc7-as3 dpb11-1 ade3::GAL-HO*) was also created by tetrad dissection of a sporulated diploid created by mating ECY413 to MY083.

***MAT* Switching Time Courses.** Single colonies were grown overnight in 3 mL yeast extract/peptone/dextrose (YPD) media at 30 °C. The following day these cultures were washed twice with 6 mL of fresh media in which dextrose was replaced with either lactate or raffinose and grown for at least 6 h. These small cultures were then used to inoculate large cultures such that they would reach a density of 0.5–1 × 10^7 cells/mL within 15 h of shaking at 30 °C. Once the cultures reached the appropriate density a T_0 sample was taken and HO was induced by adding galactose to a final concentration of 2% (wt/vol). Dextrose was added (2% wt/vol) to the cultures 1 h after galactose addition to turn HO off and allow the cells to complete the *MAT* switch.

***MAT* Switching in dpb11-1.** MY121 and MY122 *MAT* switching time courses were prepared as described above, except cells were grown overnight at 25 °C. At a cell density of ≈0.5 × 10^7 cells/mL, 1-NMPP1 (3 mM 1-NMPP1 in ethyl acetate) was added to a final concentration of 10 μM. After 5 h at 25 °C, the cultures were shifted to 37 °C for 3 h.

Southern Blotting. Genomic DNA was purified from samples of *MAT* switching cells taken at the indicated time points and then subjected to restriction digestion using the enzymes indicated in each figure. Digested DNA was separated by agarose gel electrophoresis and transferred to nylon membranes by vacuum blotting using standard procedures. Southern blots were probed with a ^{32}P-labeled *MAT* distal DNA fragment synthesized by PCR using primers AW264 and MAT10 (Table S1). All quantitative densitometric analysis was done using Bio-Rad Quantity One software. To control for differences in gDNA leaded into each lane, each fragment of interest was normalized to the *HML*α fragment, because the donor locus concentration remains unchanged throughout the time course. Each data set quantified was normalized to the time point with maximum signal, set to 100%.

Chromatin Immunoprecipitation. ChIP experiments were carried out as previously described (2) except only unpurified anti-Rad51 antibodies (gift from A. Shinohara, Osaka University, Osaka) were used in IPs. Additionally, all IPs were incubated at room temperature with antibodies and protein-G agarose beads together for 1 to 2 h before beginning washes. Some ChIP experiments were also concurrently incubated to anti-Mif1 antibodies to pull down centromeric (CEN) DNA used as internal normalizing controls.

All ChIP data were analyzed by quantitative real-time (qRT) PCR. All ChIP primer sequences are listed in Table S1. All ChIP data were normalized to either *Arg5,6* (IPs without anti-Mif1) or *CEN3* (IPs with anti-Mif1). ChIP data are presented as a ratio of ratios: either (*MAT* IP/*Arg5,6* IP) or (*MAT* IP/*CEN3* IP).

Primer Extension and NH-Tail Removal Assays. Primer extension from the right side of *MAT* and NH-tail removal were each analyzed by qRT-PCR and normalized to *Arg5,6* using the same primers described for ChIP analysis. Primer extension was detected using pA and pB (5). Removal of the NH Y**a**-tail was detected using MATXp1 and US-013 (Table S1). PCR signals for primer extension, product formation, and NH-tail removal assays were normalized to Arg5,6 as follows: T_N [assay product]/T_N [Arg5,6]. Data are represented as percentage maximum signals. The PCR signals for each time point were measured as

a fraction of the time point that gave the highest signal, which was set to 100%. Product formation/primer extension from the left side of the break was measured by qPCR using primers pC and pD (5), followed by quantitative densitometric analysis of PCR products run on 0.8% agarose gels. Each qPCR was performed with a fivefold serial dilution ladder of gDNA isolated from *MAT*α cells to assign relative concentration values to experimental samples.

Micrococcal Nuclease Assays. Strains used to measure nucleosome remodeling during *MAT* switching were JKM161, WH219, and WH259. Initiation of *MAT* switching was carried out as described above. Samples taken throughout the time courses were subjected to MNase digestion, as previously described (6), and the dynamics of nucleosome movement during DSB repair was monitored by qRT-PCR. Each qRT-PCR carried out on MNase-digested chromatin was accompanied by a 10-fold serial dilution ladder of preswitched, undigested gDNA isolated from the T_0 time point of the same time course, which was used to assign relative concentration values to the experimental samples. To control for differences in DNA concentrations across a time course, qRT-PCRs done on MNase-digested chromatin were normalized to undigested *Arg5,6* signals within a given time point. See Table S1 for primer pairs used, as well as primer sequences.

Quantitative Real-Time PCRs. For qRT-PCRs, Sigma's Jump Start Taq polymerase (D6558) was used. Reactions were supplemented with a SYBR Green mix [0.4 mM dNTPs, 20 mM Tris (pH 7.4), 0.3% Triton X-100, 1 mM $MgCl_2$, and SYBR green 1:20,000]. Each qRT-PCR was performed with a 10-fold serial dilution ladder to assign relative concentration values to the experimental samples. For primer extension assays, this dilution ladder was made from gDNA isolated from *MAT*α cells. For NH-tail removal and ChIP assay quantifications the dilution ladder was made from gDNA isolated from a preswitched isolate.

1. Lee SE, et al. (1998) Saccharomyces Ku70, mre11/rad50 and RPA proteins regulate adaptation to G2/M arrest after DNA damage. *Cell* 94:399–409.
2. Sugawara N, Wang X, Haber JE (2003) In vivo roles of Rad52, Rad54, and Rad55 proteins in Rad51-mediated recombination. *Mol Cell* 12:209–219.
3. Tong AH, et al. (2001) Systematic genetic analysis with ordered arrays of yeast deletion mutants. *Science* 294:2364–2368.
4. Yu Y, Eriksson P, Bhoite LT, Stillman DJ (2003) Regulation of TATA-binding protein binding by the SAGA complex and the Nhp6 high-mobility group protein. *Mol Cell Biol* 23:1910–1921.
5. Holmes A, Haber JE (1999) Physical monitoring of HO-induced homologous recombination. *Methods Mol Biol* 113:403–415.
6. Sekinger EA, Moqtaderi Z, Struhl K (2005) Intrinsic histone-DNA interactions and low nucleosome density are important for preferential accessibility of promoter regions in yeast. *Mol Cell* 18:735–748.

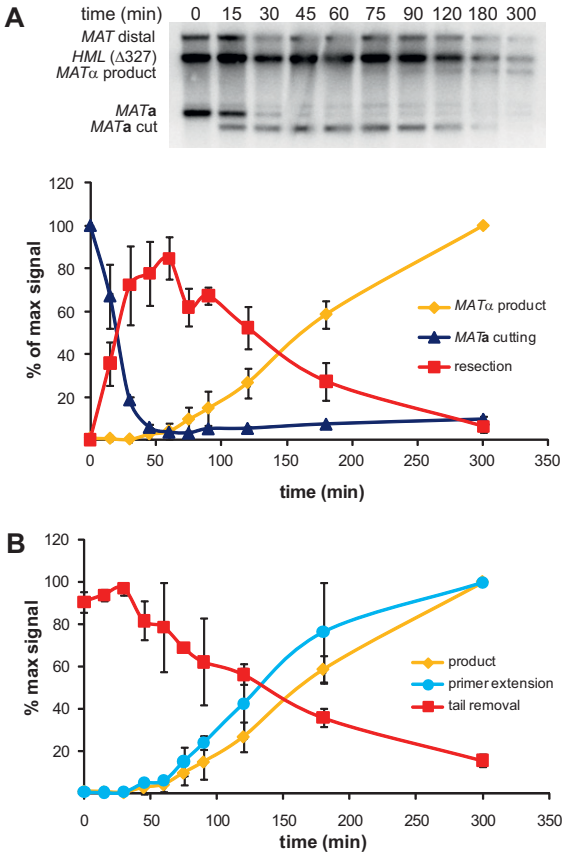

Fig. S1. Kinetics of *MAT*-switching in *HML*(Δ327) cells. (*A*) Representative Southern blot showing the progression of *MAT* switching in WH229. After HO induction, DNA was extracted at the indicated time intervals, subjected to digestion with StyI, and separated on a 0.8% agarose gel. The Southern blot was probed with a ^{32}P-labeled *MAT* distal fragment. Cells are switching from *MAT***a** to *MAT*α. Each data set is normalized to the time point with maximum signal, which is set to 100%. The graph represents quantative densitometric analysis of three Southern blots; error bars represent SEM. (*B*) Comparison of the kinetics of primer extension, NH-tail removal, and *MAT*α product formation during *MAT* switching in WH229. Each data set is normalized to the time point with maximum signal, which is set to 100%. Data represents three independent experiments; error bars represent SEM.

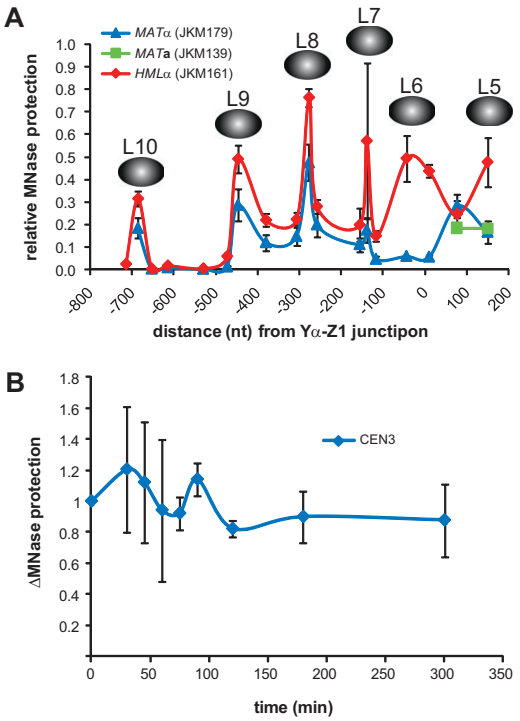

Fig. S2. (*A*) Comparison of pre-HO induction MNase protection levels at *HML*α (JKM161), *MAT***a** (JKM139), and *MAT*α (JKM179). Gray ovals represent nucleosome L5–L10 positions at *HML*. (*B*) The highly positioned nucleosomes contained within centromeres are not repositioned during *MAT* switching. These data were collected from the same normal *MAT*-switching time courses depicted in Fig. 6*B* (main text). Data for *A* and *B* represent at least three independent experiments; error bars represent SEM. MNase protection levels are normalized to untreated *ARG5,6* signals.

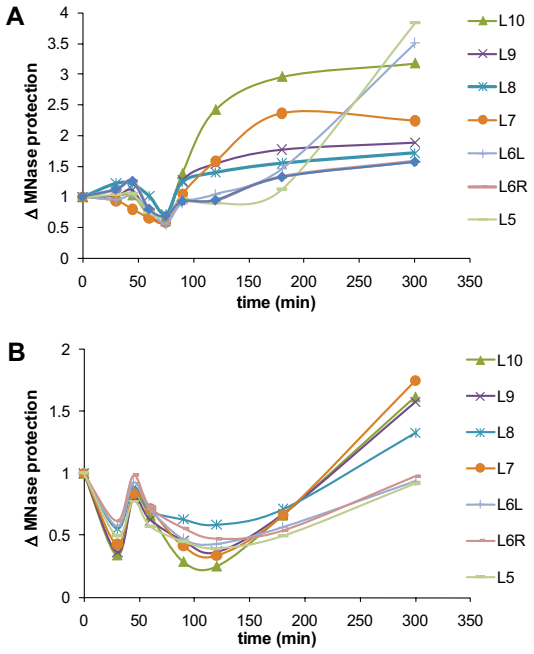

Fig. S3. Nucleosomes L5–L10 within *HML* are remodeled in a coordinated fashion during repair of a DSB at *MAT*. Graphs show fold changes in MNase protection from preinduction levels within *HML* regions protected by the indicated highly positioned nucleosomes. Samples collected during DSB repair time courses were measured by qRT-PCR. L6L and L6R represent the two protected positions (right and left) afforded by the L6 nucleosome. (*A*) Normal *MAT* switching time course. (*B*) *MAT*-BIR time course. Data for both *A* and *B* represent three independent experiments. MNase protection levels are normalized to untreated *ARG5,6* signals.

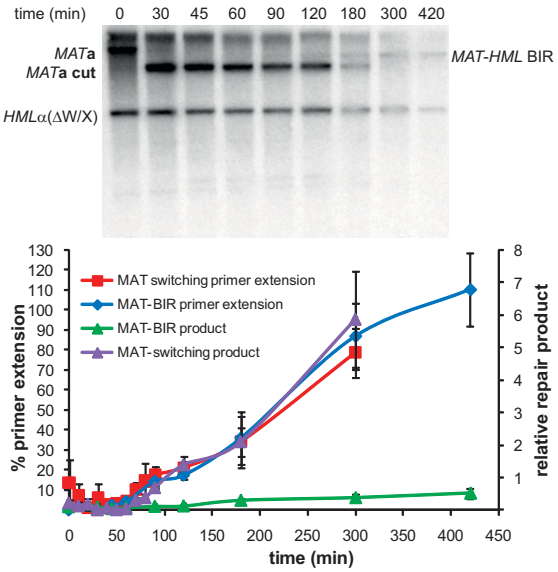

Fig. S4. Kinetics of DSB repair during *MAT*-BIR. Shown is a representative Southern blot of a *MAT*-BIR time course (WH219). After HO induction, DNA was extracted at the indicated time intervals, subjected to digestion with XhoI, and separated on a 0.8% agarose gel. The Southern blot was probed with a ^{32}P-labeled *MAT* distal fragment. Cells start out as *MAT***a**. The graph compares the kinetics of product formation and primer extension for *MAT* switching and *MAT*-BIR. Product formation data were obtained by quantitative densitometric analysis of two independent Southern blots for both *MAT* switching and *MAT*-BIR; error bars represent ranges. Primer extension data were collected from four independent *MAT*-switching experiments; error bars represent SEM, and two independent *MAT*-BIR experiments; error bars represent ranges.

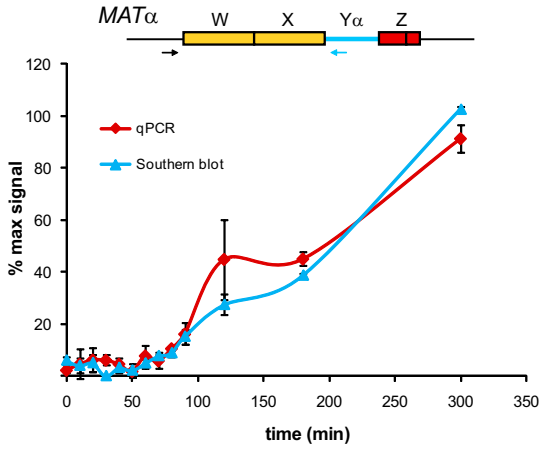

Fig. S5. Comparison of product formation kinetics during *MAT* switching in JKM161 measured by Southern blot and qPCR. Schematic shows the *MAT*α locus after repair completion. Arrows indicate the positions of primers used in qPCRs to detect product formation/primer extension from the left side of a DSB at *MAT*. qPCR data represent three independent experiments; error bars represent SEM. Southern blot data represent quantitative densitometric analysis from two independent experiments; error bars represent ranges. Each data set is normalized to the time point with maximum signal, which is set to 100%.

Table S1. Primers used for PCR analyses during *MAT* switching

Primer	Sequence (5′→3′)
HML specific qRT-PCR primers for monitoring nucleosome positions	
L5p1	CATTTGGCCTTATAGAGTGTG
L5p2	GGGGAGTTTCAAATAGGATAGC
L5p3	CACACTCTATAAGGCCAAATG
L6p2	TTTGGTTTTGTAGAGTGGTTGACGA
HOCSp3	GACAAAATGCAGCACGGAAT
HOCSp4	TCGTCAACCACTCTACAAAACCAAA
L6p1	GGGTTTATAAAATTATACTGTTGCGCGAA
L7p3	GTCTTGTCTTCTCTGCTCGC
L7p4	GCGAGCAGAGAAGACAAGAC
L7p5	CTCAGTTTCGACAGTTCAATAAGACATC
L7p2	CTGTGAGTAATATGCTCTAAAAGCCA
L7p5	As above
L7p1	CAAATTCACAGGATAGCGTC
L7p2	As above
L7p6	GACGCTATCCTGTGAATTTG
L8p1	GTCTAGCTGAGCATGTGAGG
L8p1	As above
L8p2	GAGGAAGGAACAGGAATCTGGAT
L8p2	As above
L8p3	GAACAAAGCATCCAAATCATACAGAAAC
L8p4	GTTTCTGTATGATTTGGATGCTTTGTTC
L9p1	CTCTTAACTACTTCTTTTAACCTTCAC3′
L9p1	As above
L9p2	AAACATATTGTGAATGTCGTCTATTAAG
L9p2	As above
L10p1	GCAATTTATTGCTTCCCAATGTAG
L9p3	GTGAAGGTTAAAAGAAGTAGTTAAGAG3′
L10p2	GTTCCAACATTTTATGTTTCAAAAC
L10p3	CTTCCTTTTTTTCTTGCCCAC
L10p6	GTTTTGAAACATAAAATGTTGGAAC
L10p5	GCTGGATTTAAACTCATCTGTG
L10p6	As above
L10p7	CTGGTAACTTAGGTAAATTACAGC
L10p8	GTGGGCAAGAAAAAAAGGAAG
Centromere-specific qRT-PCR primers for monitoring nucleosome positions	
Cen3p1	GTCACATGATGATATTTGATTTTATTAT
Cen3p2	TTTTAACTTTCGGAAATCAAATACAC
Cen4p1-WH	GTCACATGCTTATAATCAACTTTTTT
Cen4p2-WH	GTTTTATGTTTCGGTAATCATAAACAA
ChIP qRT-PCR primers	
Rad51 recruitment to *MAT*	
MATDp8	CGCATGGGCAGTTTACCTTT
MATZp2	CGTCTTGCTCTTGTTCCCAA
Rad51 recruitment to *HML*	
MATDp8	As above
HMLp3	AGTAGCTTTCGGATGGCACA

Table S1. Cont.

Primer	Sequence (5′→3′)
Arg5,6 normalization	
Arg5,6p1	CAAGGATCCAGCAAAGTTGGGTGAAGTATGGTA
Arg5,6p2	GAAGGATCCAAATTTGTCTAGTGTGGGAACG
CEN3 normalization	
Cen3p3	ATAATAAAATCAAATATCATCATGTGAC
Cen3p4	AATTTATCTAAATCACTCATATAAACCG
NH-tail removal qRT-PCR primers	
MATXp1	TGTTACACTCTCTGGTAACTTAGG
US-013	CCGCCATACTACAAATATCATCC
Primers used to synthesize the *MAT* distal probe used in Southern blotting analyses	
AW264	GGTGACGGATATTGGGAAGA
MAT10	GTGTTCCCGATTCAGTTTGACG

Primers are listed in the pairs used for each PCR analysis.